SENSORLESS CONTROL OF INTERIOR PERMANENT-MAGNET SYNCHRONOUS MOTOR BASED ON EXTENDED KALMAN FILTER

Laurentiu-Ionel DIACONU

"Transilvania" University of Brasov, laurentiu.diaconu@unitbv.ro

Abstract – **This paper presents a sensorless position control concept for an interior permanent magnet synchronous motor (IPMSM). Conventionally the speed of an IPMSM can be measured conveniently by d.c. tachogenerators, which are nowadays brushless d.c. tachogenerators. Rotor position can be also measured by using electromagnetic resolvers or digitally by using incremental or absolute encoders. Furthermore, an electromechanical sensor increases the system inertia, which is undesirable in high-performance drives. It also increases the maintenance requirements. In very small motors it is impossible to use electromechanical sensor. In a low-power torque-controlled drive the cost of such a sensor can be almost equal to the other costs. In drives operating in hostile environments, or in high-speed drives, speed sensors cannot be mounted. For motor spinning condition it allows estimation of rotor velocity and position of an IPMSM drive using a simple Kalman filter algorithm (EKF) with stator voltages and currents measurements. This model is more complex than the one in surface-magnet synchronous motors due to magnetic circuit asymmetry. Along with the extended Kalman filter, are presented the realized filter loop, the filter block and filter algorithm. Next, are presented the experimental results for motor starting and steady-state no-load and full-load condition in order to validate the EKF's capability to correctly estimate the system states while providing the feedback quantities to the velocity and position controllers.**

Keywords: *extended Kalman filter (EKF), interior permanent magnet synchronous motor (IPMSM), position and velocity estimation, sensorless drive.*

1. INTRODUCTION

To reduce total hardware complexity and costs, to increase the mechanical robustness and reliability of the electrical drives, and to obtain increased noise immunity, it is desirable to eliminate electro-mechanical sensors in vector controlled and direct torque controlled drives.

Great efforts ([1] – [8]) have been made to introduce speed and/or shaft position sensorless torque controlled (vector and direct torque controlled) drives. The terminology 'sensorless' refers to only the speed and shaft sensors: there are still other sensors in the drive system (e.g. current sensors), since closed-loop operation cannot be performed without them.

2. EXTENDED KALMAN FILTER

The basic idea in defining an extended Kalman filter consists in the relinearization around every state estimation $\hat{X}(k)$ immediately after being calculated at the corresponding t_k. Just after achieving a new state estimation, the nominal state trajectory is improved and introduced into the algorithm. This enhances the validity of the assumption by which the deviation from the reference trajectory is sufficiently small so as to allow the application of the linearization techniques of perturbations with optimum results.

Suppose the system described through its dynamical model [3]:

$$\dot{X}_n = f\left[X_n(t), U(t), t\right] + G(t)W(t) \tag{1}$$

$$Y(k) = h\left[k, X(k)\right] + V(k)$$

The algorithm of the extended Kalman filter includes the measured quantities $Y(t_k)$ by means of the equations [3]:

$$K_k = P_k H_k^T\left[k, \hat{X}^-(k)\right] \times \left(H_k\left[k, \hat{X}^-(k)\right] P_k^- H_k^T\left[k, \hat{X}^-(k)\right] + R_k\right)^{-1}, \tag{2}$$

$$\hat{X}(k) = X^-(k) + K_k\left[\hat{Y}(k) - H_k\left[k, X^-(k)\right]\right], \tag{3}$$

$$P_k = \left(I - K_k H_k\left[k, \hat{X}^-(k)\right]\right) P_k^-, \tag{4}$$

where $H_k\left[k, \hat{X}^-(k)\right]$ is defined as the *mxn* order matrix of the partial derivatives:

$$H_k\left[k, \hat{X}^-(k)\right] = \frac{\partial}{\partial X} h\left[X, k\right]\Big|_{X = \hat{X}^-(k)} \tag{5}$$

The estimation is propagated forward, toward the next sampling instant *k+1* by integrating the equations:

$$\dot{\hat{X}} = f\left[\hat{X}(t), U(t), t\right] \quad (6)$$

$$\begin{aligned}\dot{P}(t) &= \Phi\left[t, \hat{X}(t)\right]P(t) + \\ &P(t)\Phi^T\left[t, \hat{X}(t)\right] + G(t)Q(t)G^T(t)\end{aligned} \quad (7)$$

from time t_k to t_{k+1}, by using initial conditions provided by equations (3 and 4).
The temporal propagation relations can be equivalently written as:

$$\hat{X}^-(k+1) = \hat{X}(k) + \int_k^{k+1} f\left[\hat{X}(t), U(t), t\right]dt \quad (8)$$

$$\begin{aligned}P^-(k+1) &= \Phi\left[k+1, k, \hat{X}\right]P(k)\Phi^T\left[k+1, k, \hat{X}\right] + \\ &+ \int_k^{k+1} \Phi\left[t, \hat{X}\right]G(t)Q(t)G^T(t)\Phi^T\left[t, \hat{X}\right]\end{aligned} \quad (9)$$

Notably, the matrices Φ, *H*, *K* and *P* are evaluated knowing the most recent estimated value of the nominal state trajectory. Consequently, the equations of propagation and recalculation of the covariance of the estimation error are coupled with the state estimation relations. The covariance and amplification Kalman matrices cannot be calculated a priori without knowing state estimation and the currently measured values, as well.

3. THE KALMAN FILTER ALGORITHM

The most important aspect for a precision simulation is a perfect separation between the continuous process and the discrete one within the complete system. The Kalman algorithm and the control algorithm are the discrete components of the process, while the inverter and motor operation are the continuous components. Therefore, the first step in designing the Kalman filter consists in introducing an additional block which considers the sample-hold process of the continuous quantities acquired from the continuous system. This block is named *Unit Delay* (z^{-1}) and is intended for the sampling of all vector components applied to its input at regular intervals, set by the sampling period, holding the acquired value until a new sampling arrives (Fig. 1 – "vsa", "vsb", "isa" , "isb" are the measured voltages and currents respectively in the stator phases).

Apart from current and voltage sampling, *Unit Delay* also provides sampling of the output vector of the estimated states. Thus, to the Kalman filter will be introduced 9 discrete input signals, which are modified every T_s sec. (T_s is the sampling period).

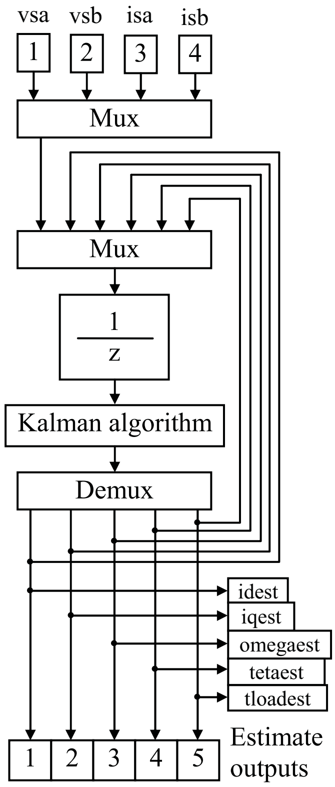

Figure 1: Kalman filter block

To obtain a clear picture on the Kalman filter algorithm and on the way it was constructed, we present in the following the logical diagram of the algorithm. By examining the logical diagram in Fig. 2, we notice that the state vector estimated at time *k+1* depends on the previous measurements and estimations, considered at time *k*. Therefore, the measured quantities and the current estimations are introduced into the *Kalman algorithm* block delayed by one sampling step.
The *Mux* and *Demux* blocks are intended for combining and respectively decomposing the input quantities into vector quantities and into their components as well.
The Kalman algorithm included in the *Kalman algorithm* block is designed as a common Matlab function (*M-Function*) which returns the current estimation vector and the covariance matrix *P* at every sampling period. While the estimates are reintroduced directly at the input, the covariance matrix is defined as a global variable updated at a every iteration.
The Kalman filter's mathematical model is given by:

$$\begin{bmatrix} i_{sd} \\ i_{sq} \\ \omega \\ \theta \\ m_s \end{bmatrix}_{k+1} = \begin{bmatrix} -\frac{r_s}{L_d} i_{sd} + \omega \frac{L_q}{L_d} i_{sq} + u_{s\alpha} \cos\theta \frac{1}{L_d} + u_{s\beta} \sin\theta \frac{1}{L_d} \\ -\omega \frac{L_d}{L_q} i_{sd} - \frac{r_s}{L_q} i_{sq} - \omega \frac{\Psi_f}{L_q} - u_{s\alpha} \sin\theta \frac{1}{L_q} + u_{s\beta} \cos\theta \frac{1}{L_q} \\ \frac{3p^2}{2J}\left(L_d - L_q\right) i_{sd} i_{sq} + \frac{3p^2}{2J} \Psi_f i_{sq} - \frac{B}{J}\omega - \frac{m_s}{J} p \\ \omega \\ m_s \end{bmatrix}_k + w(t_k) \tag{10}$$

where the state variable are i_d, i_q, ω, θ and m_s (i_d and i_q are current space vector components in rotor reference frame; ω - rotor electrical speed; θ - rotor position; m_s - load torque), v_α and v_β are voltage vector components in the stator reference frame.

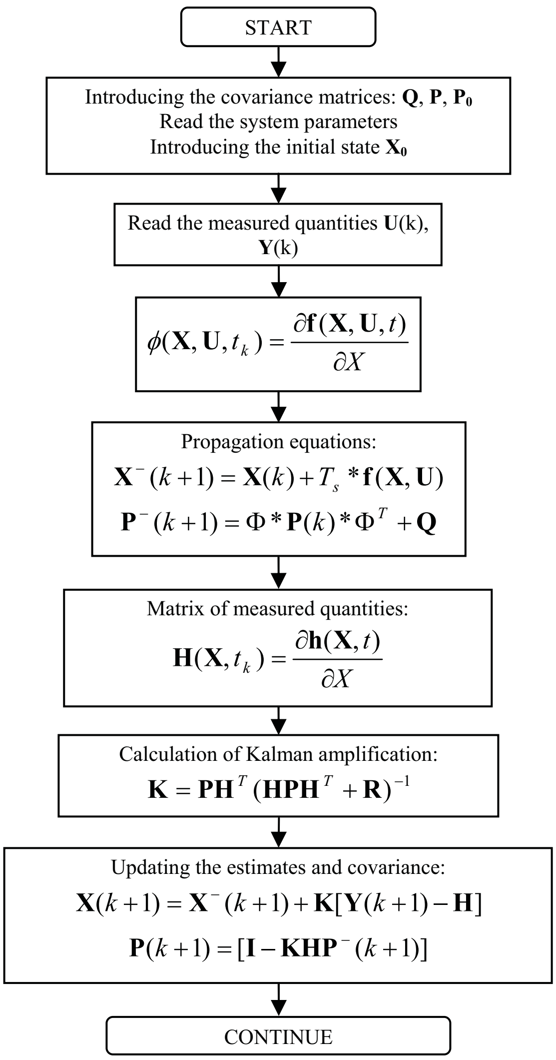

Figure 2: Simplified block diagram of the Kalman filter algorithm

The load torque m_s is a state mechanical variable with slowly variation and it can be considered constant during one sampling period. $W(t)$ is a process noise which take into consideration the modeling errors (nonlinears, saturations, a.s.o.), noise which is introduced to the measurement elements and parameters variations around about mean value.

A critical part of the design of EKF is to use correct initial values for the various covariance matrixes , Q, R, and P. the system noise covariance Q accounts for the model inaccuracy, the system disturbances, and the noise introduced by the voltage measurements (sensor noise, A/D converter quantization).

The noise covariance R accounts for measurement noise introduced by the current sensors and A/D quantization.

The initial state covariance P_0 can be assumed diagonal and the elements of first diagonal are the mean-square error to knowledge the initial conditions.

For P_0, Q, and R matrices was used the following values:

$$Q = \begin{bmatrix} 5e-4 & 0 & 0 & 0 & 0 \\ 0 & 5e-4 & 0 & 0 & 0 \\ 0 & 0 & 5e-4 & 0 & 0 \\ 0 & 0 & 0 & 5e-4 & 0 \\ 0 & 0 & 0 & 0 & 5e-4 \end{bmatrix}$$

$$P_0 = \begin{bmatrix} 5e-4 & 0 & 0 & 0 & 0 \\ 0 & 5e-4 & 0 & 0 & 0 \\ 0 & 0 & 5e-4 & 0 & 0 \\ 0 & 0 & 0 & 5e-4 & 0 \\ 0 & 0 & 0 & 0 & 5e-4 \end{bmatrix}$$

$$R = \begin{bmatrix} 0.01 & 0 \\ 0 & 0.01 \end{bmatrix}$$

The motor parameters are: $p = 2$, $r_s = 0.57$ ohm, $\Psi_f = 0.108$ Wb, $L_d = 8.72$ mH, $L_q = 22.8$ mH, $V_{sm} = 100$ V, $i_{sm} = 10$ A, $\omega_N = 200$ rad/s.

4. SIMULATIONS RESULTS

The dynamical behavior of the motor is obtained by solving the differential equations of the machine by using the Runge-Kutta of order 4 integration method along with Euler's integration method. Both methods have generated similar results, but the simulations time in the second case is generally much shorter than in the first one. The input quantities of the motor model are the phase voltages generated by a hysteresis current controller of PWM-type. All tests were performed in closed loop.
In the following, we shall present some significant results for different operating modes.

4.1. Starting and no-load operation at 150 rad/s.

Both the motor and the Kalman estimator are started from standstill, while the motor is accelerated to the desired speed of 150 rad/s (Fig.3).

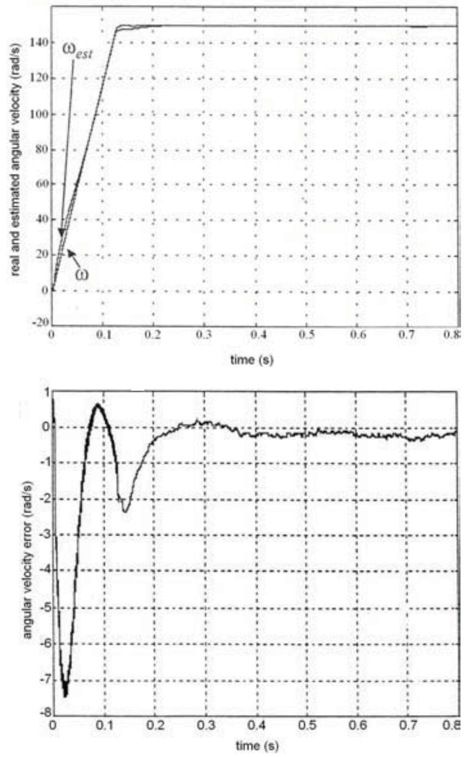

Figure 3: a) Variation of real angular velocity and of estimated velocity at no load starting and stady-state running (150 rad/s)
b) Angular velocity error at starting and steady-state.

The initial speed value is zero and the motor is supposed to start with an initial flux angle of 0 degrees. During functioning no load torque is applied and the friction torque is neglected. Also, no variation of motor parameters occurs during functioning.

We notice that the Kalman filter correctly estimates the angular velocity at non-load operation. The most important velocity error is obtained during the starting process, when the absolute value difference between real angular velocity and the estimation one is of approximately 7 rad/s, which represents an error of 4.6%. It can be observed that the estimated velocity is higher than the real one due to the larger initial error of load torque estimation.
The Kalman filter estimates a negative load torque at the shaft during the first 10 ms which would mean that the motor is driven externally from its shaft. However, after initiating the Kalman filtering process, the estimated load torque approaches its real value determining the estimated velocity to approach the actual shaft speed. The first settling time of the transient process is about 20ms after which the operation settles.
The load torque converges at the expected value of 0 Nm and the estimated angular velocity is kept, with negligible error at real velocity value.
Notably, the drive is controlled by using as feedback quantity precisely this estimated angular velocity with the desired outcome, that is, operation with a steady-state error below 1%. At the same time, for calculating the current references of the hysteresis controllers from the mobile system into the fixed system, we used the estimated angle $\hat{\theta}$. The estimation error is presented in Fig. 4b.

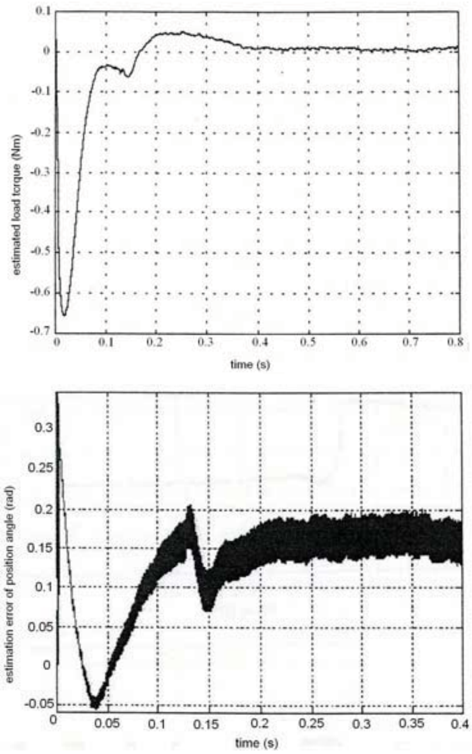

Figure 4: a) Estimated load torque at staring and no-load steady-state running ;
b) Estimation error of position angle.

We notice a constant steady-state error of about 0.16 rad which is reflected only as a steady-state velocity error.

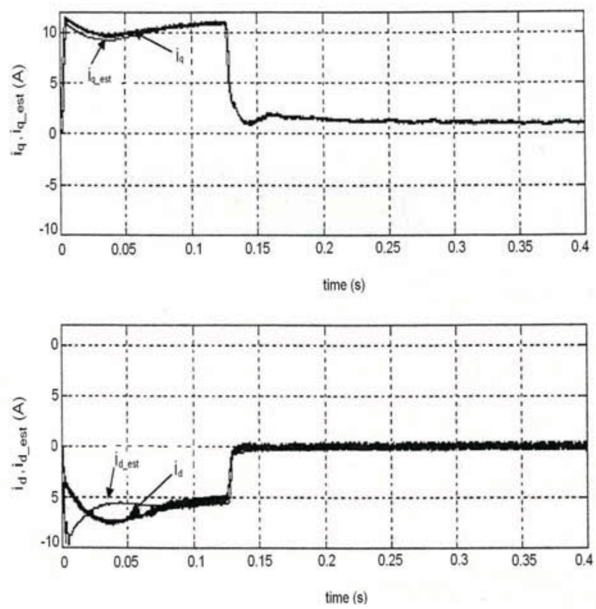

Figure 5: Real and estimated components of the stator currents.

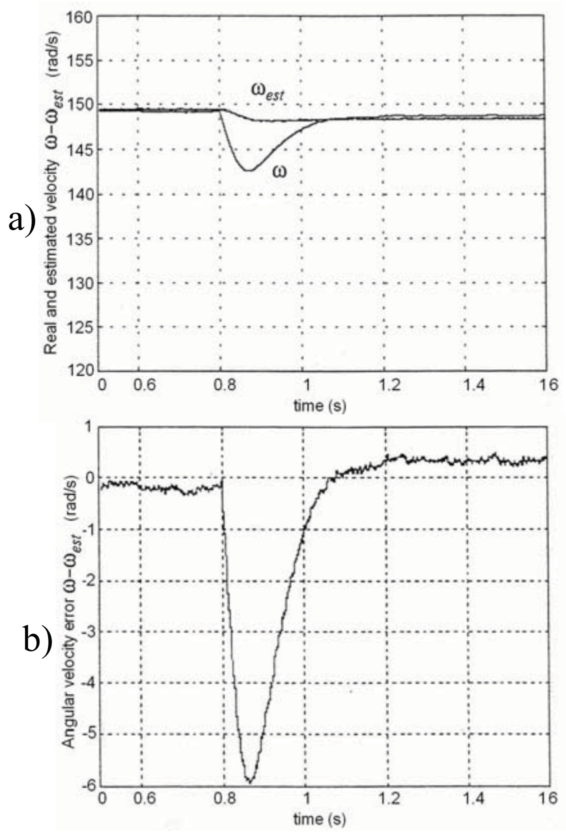

Figure 6: a) Real and estimated velocity when appling a load torque;
b) Angular velocity error for applied step

The sampling period for this first set of simulations was set to 400µs, which is considered to be sufficient to allow the signal processor to perform the calculations.

Figure 5 presents the transversal and longitudinal components of the stator currents.

We used the control algorithm, presented previously, which calculates both current components by means of maximum torque per ampere zones and field reduction. The feedback quantities of the current computing blocks are the currents estimated with the angle $\hat{\theta}$. If we compare these currents $\hat{i}_{sd}$ and $\hat{i}_{sq}$ with the real ones from the model of the motor, we notice the fact that the Kalman filter correctly follows the current components as well, but with a certain error in the interval 0 – 0.1s when the filter seems to experience a self-tuning process.

4.2. The 0.9 Nm torque step applied during steady-state running at 150 rad/s.

In this situation, the motor and the Kalman filter operate at steady-state, at a velocity of 150 rad/s. After 0.8 s, a 0.9 Nm load torque is applied to the motor shaft. The Kalman filter is unaware of the applied load torque but detects the perturbation arising within the system through the magnitude of the system's covariance matrix. Consequently, the Kalman amplification increases and tries to minimize the observed estimation error. The real velocity of the motor decreases faster since the load torque acts instantaneously on the motor shaft (Fig. 6 and 7).

The Kalman filter is slower than the real process. Firstly, the state quantity which corresponds to the load torque begins to increase. The results are a gradual decrease of the estimated speed, while the effect observed in the speed controller is an increased reference in the transversal component of the current i_q^*. This component will increase continuously until the estimated load torque reaches the steady-state value (0.9 Nm – Fig. 8)

Meanwhile, the real speed is amplified due to the arising electromagnetic torque subsequent to the increase of the transversal current.

The electromagnetic torque tends to equate the load torque and the speed will be resettled to its initial value (with a certain steady-state error).

5. CONCLUSIONS

This paper presents an EKF for the sensorless control of an IPMSM. Departing from the linearized Kalman filter, we obtained the extended Kalman filter. In comparison with other papers [5-9], we introduce a novel supplementary state – load torque.

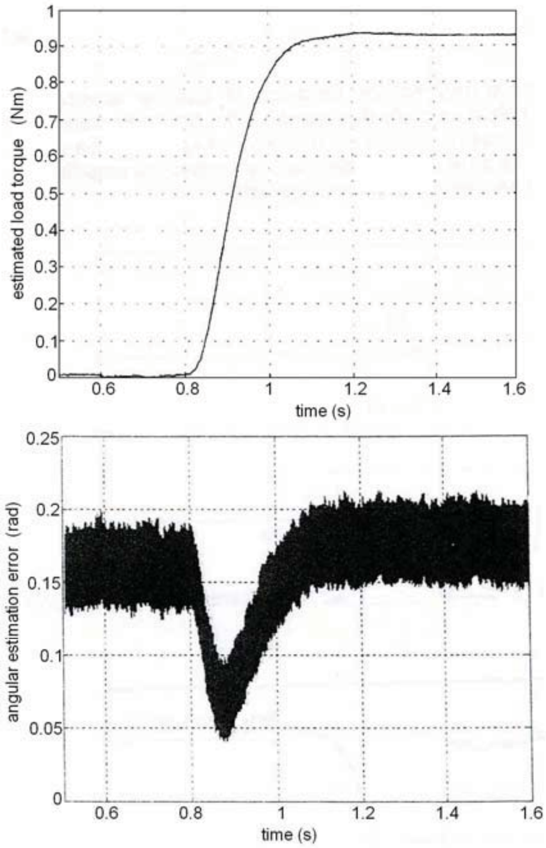

Figure7: a) Estimated load torque when applying a real torque of 0.9Nm at time 0.8s;
b) Angular estimation error at load torque.

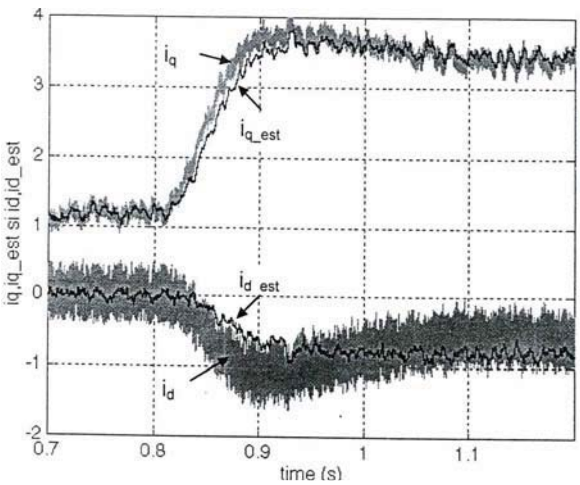

Figure 8 : Real and estimated current components at step torque.

The estimation of this variable - when it is include to the state space and therefore in the system matrix (see equation (10)) - give a high improvement to the estimation of the mechanical behavior of system.

Using proposed filtering algorithm we have simulated and verified, at no-load and at full load, the capability of the filter to correctly estimate the control system states of the IPMSM.

The load torque has been estimated as well, an aspect which is less known from technical literature.

References

[1] B. Gallwitz, F. Hillenbrand, *A proposal for Avoiding the Direct Measurement of Speed and Angular Position of the Synchronous Machine*, IFAC control in Power Electronics and Electrical Drives, Laussane, Switzerland, 1983;

[2] U. Kirkberg, Ph. Sattler, *State Estimation of an Inverter fed Synchronous Motor*, EPE'96, Brussels, October 1986;

[3] R. Dhaouadi, N. Mohan, L. Norum, *Design and Implementation of an Extended Kalman Filter for State Estimator of a Permanent Magnet Synchronous Motor*, IEEE Annual Meeting Conference Record, June, 1990;

[4] B.J. Brunsbach, G. Henneberger, *Position Controlled Permanent Excited Synchronous Motor without Mechanical Sensors*, EPE'93, Bringhton, U.K., 1993.

[5] S. Nakashima, I. Inagki, I. Miki, *Sensorless Initial Rotor Position Estimation of Surface Permanent Magnet Synchronous Motor*, IEEE Trans. Ind. Appl., vol. 36, Nov./Dec., 2000, pp. 1598-1603.

[6] M. Tursini, R. Petrella, F. Parasiliti, *Initial Rotor Position Estimation Method for PM Motors*, IEEE Trans. Ind. Appl., vol.39, Nov./Dec. 2003, pp.1630-1640.

[7] H. Kim, K.K. Huk, R.D. Lorenz, T.M. Jahns, *A Novel Method for Initial Rotor Position Estimation for IPM Synchronous Machine Drives*, IEEE Trans. Ind. Appl., vol.40, Sept./Oct. 2004, pp.1369-1378.

[8] J.I. Ha, K. Ide, T. Sawa, S. K. Sul, *Sensorless rotor position estimation of an interior permanent magnet motor from initial states*, IEEE Trans. Ind. Appl., vil. 39, no. 3, 2003, pp. 761-767.

[9] M.E. Haque, L. Zhong, M.F. Rahman, *A sensorless initial rotor position estimation scheme for direct torque controlled interior permanent magnet synchronous motor drive*, IEEE Trans. Power Electron., vol. 18, no. 6, 2003, pp. 1376-1383.